Proceedings of the
9th Graz Brain-Computer Interface Conference 2024
10.3217/978-3-99161-014-4-093

EEG CORRELATES OF ERROR-RELATED ACTIVITY DURING BALLISTIC COMPUTER MOUSE MOVEMENTS

Idorenyin Amaunam[1], Mushfika Sultana[1], Borja Rodriguez-Herreros[2], Tej Tadi[3], Robert Leeb[3], Serafeim Perdikis[1]

[1]Brain-Computer Interface and Neural Engineering Laboratory, School of Computer Science and Electronic Engineering, University of Essex, United Kingdom
[2]Service des Troubles du Spectre de l'Autisme et apparentés, Département de psychiatrie, Lausanne University Hospital (CHUV), Lausanne, Switzerland
[3]Mindmaze SA, Lausanne, Switzerland
E-mail: ia21792@essex.ac.uk

ABSTRACT: It has been repeatedly shown that processing of perceived errors in the human brain may elicit some type of evoked response in electroencephalography (EEG) collectively termed as Error-Related Potential (ErrP). The study of ErrP signatures offers a potential back door to better understanding how the brain encodes and reacts to errors and a useful tool for poking adaptation and learning, but also has several practical applications in Brain-Computer Interface (BCI) and general Human-Computer Interaction (HCI). The bulk of this literature has focused on so-called "interaction" ErrP, reflecting the response to discrete events occurring during self-paced, casual interaction of a subject with their environment. Here we present a two-case study investigating the existence and characteristics of ErrP EEG correlates in an eye-hand coordination task consisting in "ballistic" computer mouse movements, where the action and reaction time constraints imposed on the subject are extremely tight. We show that clear EEG substrates of error processing can be retrieved for both subjects and bare strong similarities with the interaction ErrP waveforms. The findings of this work suggest the possibility of detecting, in real-time, errors committed during fast-paced interaction, thus potentially enabling automatic ErrP-based error correction in real-world BCI and HCI scenarios.

INTRODUCTION

Error-Related Potentials (ErrPs) are Event-Related Potential (ERP) waveforms in EEG time-locked to the realization of committed errors [1]. Mainly owing to its utility as an automatic, subconscious means of error correction during BCI [2] or general HCI, the topic of ErrP signatures in various contexts has been extensively studied in the last 20 years [3]. ErrP correlates are relatively slow signals characterized by a negative fronto-central peak around 100 ms after the error onset, and followed by a larger, positive, centro-parietal peak with latency about 500 ms, which has been associated with the subject's awareness of the error [1, 4]. Based on source imaging and localization studies, ErrP correlates are believed to originate in the anterior cingulate cortex [1, 4].

Besides the inherent interest of cognitive neuroscience in ErrPs as a means to elucidate the brain's error processing mechanisms [1, 5], ErrP detection has attracted a lot of attention due to a wide spectrum of promising applications in BCI and HCI. First and foremost, ErrP recognition offers a seamless avenue for automatic error correction in human-machine interfaces [6, 7] that requires no direct manual intervention by the user [3]. In particular, this is convenient for BCI applications where EEG or other brain signal monitoring is already available to support the main interface control modality [8–14], so that ErrP detection yields no additional burden for the system's apparatus. As ErrPs are a natural physiological "reward"/punishment signal, they have also been used in the context of BCI human-machine co-adaptation [15], especially with respect to reinforcement learning approaches [16–18]. Interestingly, under the same framework ErrPs may also play the role of the main BCI modality [19, 20]. In order to optimize such applications, a lot of studies have been dedicated to the design of machine learning and other techniques for enabling high-accuracy single-trial classification of ErrP correlates, overcoming various engineering challenges [4, 12, 21–23].

The aforementioned prototypical error-related pattern is commonly observed in experimental protocols involving "discrete" errors of the interface that clearly constitute single events: there is an abrupt, profound error onset to which the ErrP signal is time-locked, and the duration of the erroneous action or feedback are relatively short [4, 11, 23, 24], even when such errors are embedded in continuous interaction and unpredictable feedback tasks [6, 12, 14, 25, 26]. Very few investigations have been carried out with regard to gradually unfolding errors [27]. However, despite the similarities of extracted ErrP waveforms in this regular discrete ErrP category, important differences or even complete absence of ErrPs have been denoted depending on the particular task (e.g., interaction, response, or observation [3]) and contextual circumstances [24] of the experimental design.

As previously argued [1], a critical factor in the elicita-

Published by
Verlag der Technischen Universität Graz

10.3217/978-3-99161-014-4-093

tion and shape of ErrPs may be the time constraints imposed on a human subject when requested to detect errors. Notwithstanding the fact that many of the studies in this literature yielded high mental workload for the user during the error recognition task induced by concurrent observation or interaction tasks, typically, the amount of time available to consolidate the occurrence of an error is ample. Here, we aimed to investigate whether ErrP signatures can be elicited and captured in EEG activity when errors happen while human individuals are engaged in an extremely fast-paced eye-hand coordination activity.

The elegance and efficiency of human movements owes much to our ability to compensate for inaccuracies and environmental perturbations. Performing online corrections relies on real-time monitoring of the hand/body trajectory from the onset of the movement [28]. We devised an experimental protocol with two related but distinct goals: (i) to assess the facilitatory effects of excitatory neuromodulation, specifically, anodal high-density transcranial Direct Current Stimulation (tDCS) [29] of the intraparietal sulcus on visuo-motor coordination, and (ii) to determine the existence and features of ErrP with simultaneous EEG monitoring, while subjects are asked to perform a "double-step" reaching task. Here, we provide preliminary analysis on the second goal of describing potential EEG correlates of error perception in this protocol.

Online eye-hand coordination has often been investigated via double-step reaching tasks, in which the target of a reaching movement suddenly moves to a new location after the movement onset and subjects are asked to adjust the movement trajectory to compensate for the perturbation. In the present study, subjects were required to put the computer mouse pointer into a narrow circular target at the top of the screen starting from a base location at the bottom with "ballistic" movements, as accurately and, very importantly, as fast as possible, with maximum possible velocity and acceleration. We hypothesized that target displacement during ballistic movements may evoke ErrP waveforms and seek to describe them. Our preliminary results with two subjects confirm this hypothesis and suggest that, despite the task's extreme timing demands, the elicited error-related responses resemble the interaction ErrPs identified in the literature. We further show that trials with target displacement can be identified with a shallow classifier, opening the road for enriching naturalistic interaction with elaborate error detection and correction capabilities even for hurried tasks.

MATERIALS AND METHODS

Participants:

We report on two subjects, S1 and S2, randomly picked for initial analysis from a larger dataset of 28 healthy right-handed volunteers (11 female; mean age 24.9 $\pm$ 5.8 years). All participants were naïve with respect to the experimental procedures and the hypothesis of the study. Participants had normal or corrected-to-normal visual acuity and reported no history of neuropsychiatric disorders. Prior to their inclusion in the study, participants signed written informed consent. The study was performed according to the declaration of Helsinki and was approved by the local Ethics Committee. All participants were screened for HD-tDCS tolerance [29]. The Edinburgh handedness inventory was administered to assess handedness.

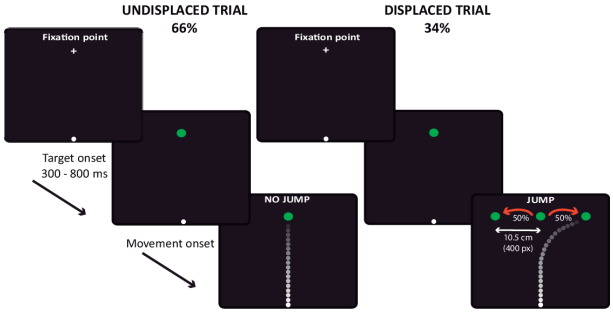

Figure 1: Experimental protocol. Trial timeline and illustration of the protocol's events and visual elements.

Experimental setup and protocol:

Participants were seated in front of a table positioned 45-50 cm below their eyes. Visual stimuli (see below) were generated using Python v3.6 running on Windows 10 in an Intel Core i7-7700 3.6 GHz computer and displayed on a 24" HP E232 monitor with a refresh rate of 60 Hz and a resolution of 1920x1080 pixels. A high-speed Logitech G G203 prodigy cable mouse, sampling at 250 Hz, was used to track the hand's 2D spatial position during reaching movements.

EEG data were recorded at 500 Hz sampling rate with a Starstim 8 hybrid EEG/tDCS 8-channel, active, wet, Ag/AgCl electrode system (Neuroelectrics, Barcelona, Spain). We measured positions FCz, FC1, Cz, CP1, CP5, P3, PO3 and PO7 of the 10-20 EEG localization system. This channel montage was designed to satisfy and compromise the needs of both the goals set during the study's design, including the possibility to focally excite the intraparietal sulcus through tDCS. Enough, strategically placed electrodes covering fronto-central and parietal cortical areas were included to capture ErrP activity.

Each subject executed 3 experimental sessions, which consisted of 5 runs each. Each run lasted approximately 6 minutes, and included 100 trials performed with the subject's dominant hand, for a total of 1500 trials per subject. Subject S1 of this study exectuted an additional 3 sessions of 3 runs each, for a total of 2400 trials. The experimental task consisted in performing a fast goal-directed reaching movement towards a visual target located in the center of the screen (Fig. 1). Prior to the initiation of the trial, participants were required to move the mouse to the starting position in the bottom center of the screen. After 1000ms with the mouse placed at this starting point, a small white fixation cross was automatically shown as a warning signal in the centre of the screen. The fixation cross preceded the target onset by a variable period (300 or 800ms) to avoid participants from predicting the timing of that onset. Trials with (34%) and without (66%) target dis-

Published by
Verlag der Technischen Universität Graz

10.3217/978-3-99161-014-4-093

placement were presented in pseudo-random order. In non-displaced trials, the target remained static in the center of the screen. In displaced trials, however, the target showed an unexpected 10.5cm (400 pixels) lateral displacement–disappeared and instantly re-appeared to the left or to the right with a 50-50% chance-, after the initiation of the reaching movement. The movement onset was detected by a 50 mm/s velocity threshold of the mouse movement. The target displacement was timed exactly at the movement onset (maximum 6 ms delay due to technical limitations of the experimental protocol) to assure that participants did not have relevant visual cues about the final position of the target during the initial movement planning.

The total longitudinal distance between the starting point and the target was 30 cm (1200 pixels) in the screen. The ratio between the distance travelled by the mouse in the real world and the cursor in the screen was 2:3, that is, when the mouse moved for example by 20 cm, the cursor advanced by 30 cm in the screen. To discard trials with long reaction times, a warning sound was provided when the velocity threshold required to start the movement was not reached during the 500 ms that followed the target onset. Participants were instructed to hit the target as fast and as accurate as possible performing a ballistic movement, exhibiting maximum velocities and accelerations over a very short period of time. When the target was displaced, participants had to adjust their hand trajectory to succeed in hitting the target in its final location. The target was presented for 1000 ms. At the end of the reaching movement, participants brought their hand back to the starting point, and prepared to start the next trial. Participants were instructed not to move their trunk with respect to the chair and avoid head movements.

Data Analysis and Evaluation:

EEG data were band-passed with a 3^{rd}-order Butterworth filter within [1-20] Hz to remove signal drifts and isolate the spectral range within which ErrP components are known to be found [7]. The final epochs considered for analysis corresponded to the trial segment [-1, 1] s where $t = 0$ s the movement onset. Subsequently, automatic artifact removal with FORCe [30] and DC removal baselining were applied to each epoch. Finally, we removed all epochs whose maximum filtered amplitude exceeded 100 μV. We assessed the statistical significance of the difference in amplitude among trials of a subject with (Error) and without (Correct) displacement through two-sided, unpaired t-tests with $a = 0.05$ and Bonferroni correction for multiple ($N = 8000$, 8 channels $\times$ 1000 time points) comparisons. Two-class (Correct vs Error) classification accuracy is derived with 10-fold cross-validation employing a binary Decision Tree (DT) classifier. DT is selected for a first attempt to classify these novel ErrPs as less vulnerable to overfitting and class-bias than other shallow models (including linear or quadratic discriminant analysis with regularization/shrinkage), taking into account the fact that there are double Correct than Error trials in the dataset. The 100-best, in terms of r^2 feature fitness, spatio-temporal (i.e., chanel/time-point combinations) amplitude features are selected using the fold's training data. Average and standard deviation (across folds) of the total and class-wise classification accuracy are reported per subject.

RESULTS

We present results on 2306 trials of S1 and 1494 trials of S2 that survived the trial rejection. Fig. 2 and 3 establish beyond doubt both the elicitation of evoked potentials during the performance of this protocol's task, and the fact that pronounced and statistically significant differences exist between Correct (with no target displacement) and Error (with target displacement) trials. The grand average waveforms are consistent across subjects.

Correct trials (blue) exhibit a large positive peak around $t = 500$ ms from movement/displacement onset ($t = 0$ ms), followed by a very small "refractory" negative peak at $t = 680$ ms for S1; this is completely absent for S2. Early negative peaks can be also identified around $t = 260$ ms, especially for S2 and for Error trials. On the other hand, Error trials (red) show a similar shape, which is however delayed: the large positive peak is located around $t = 600$ ms and the refractory negative peak around $t = 750$ ms for S1 and slightly before $t = 1.0$ s for S2. As a result, the average difference Error-Correct (black) demonstrates a first negative peak at $t = 500$ ms (very consistently for both subjects) ahead of a larger positive peak in the interval $t = [650, 720]$ ms. The differences Correct versus Error are statistically significant in the period $[400 - 800]$ ms that includes both the negative and the positive peak, for both subjects; there are no significant differences outside this interval (apart from few very short, spurious ones), which further points to the observed effects corresponding to ErrPs.

The grand average difference between Correct and Error trials is very similar to that reported in the literature for interaction ErrP in different contexts [1, 4, 7, 11, 12]. Along the same lines, Fig. 4 shows that the derived waveform, despite being fairly spread for both subjects, is stronger in fronto-central (channels FCz, Cz) and to a lesser extent parietal (PO3) regions, and is not particularly lateralized (i.e., the phenomena fade out for peripheral channels), which also aligns well with the findings of previous studies on ErrPs.

Fig. 5 shows that above-chance classification accuracy can be obtained for S1 and S2 with a DT classifier discriminating Error from Correct trials. However, the classification is biased towards the dominant Correct class, and only half of the ErrPs can be identified correctly.

DISCUSSION

The results confirm both the generation of evident ErrP EEG correlates in the framework of this protocol, and that these are similar to interaction ErrPs. However, significant differences are also noted. In particular, while

Published by
Verlag der Technischen Universität Graz

10.3217/978-3-99161-014-4-093

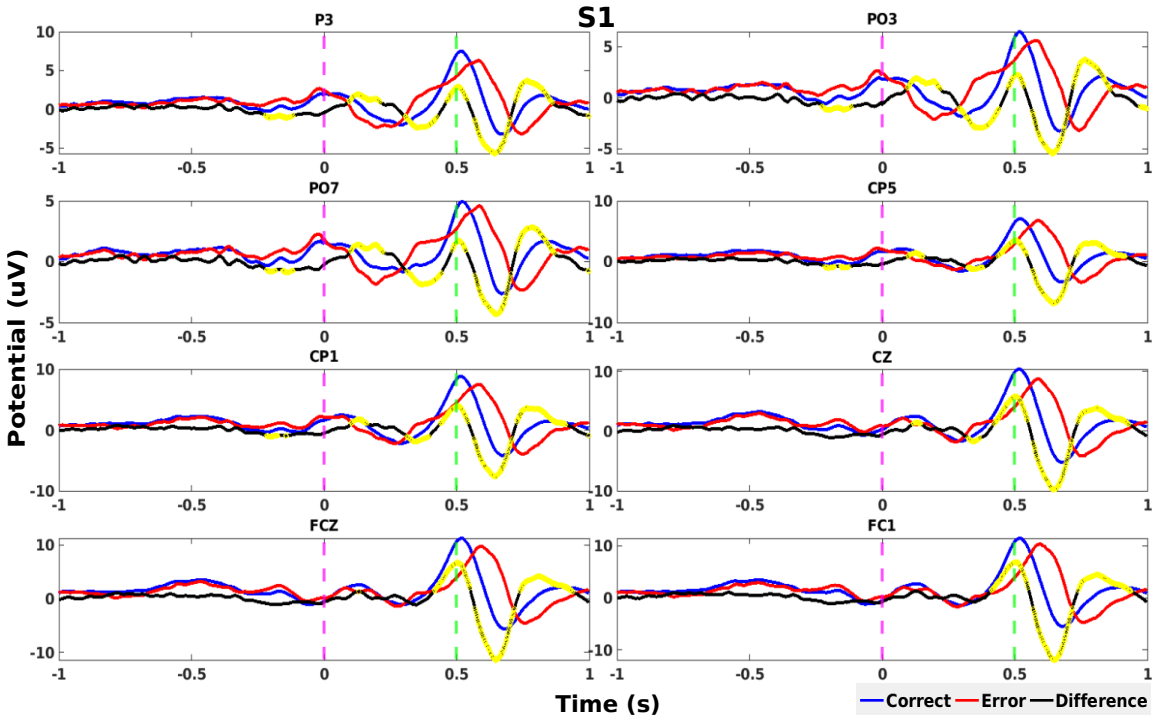

Figure 2: Grand averages of S1 trials. Correct trial average in blue, Error in red. The black line illustrates the difference Error-Correct. Vertical, dashed lines indicate salient time points: magenta for $t = 0$ ms (basllistic movement onset) and green for $t = 500$ ms. Yellow circles illustrate statistically significant difference between Error and Correct amplitudes for this time point.

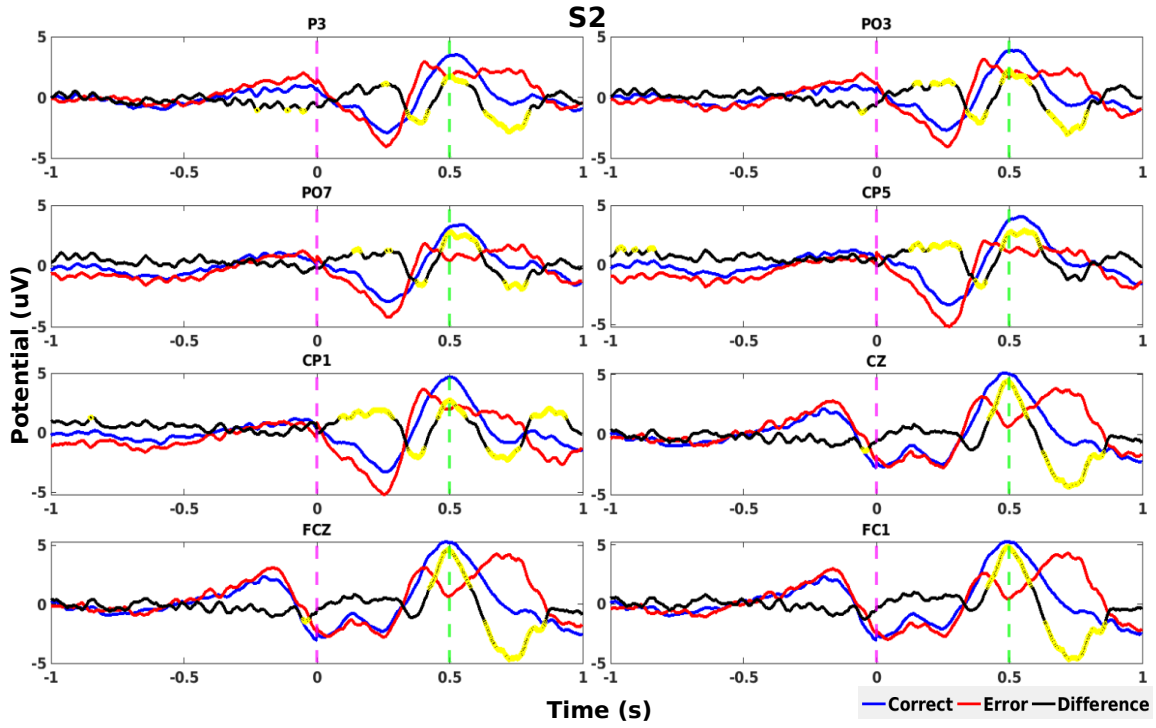

Figure 3: Grand averages of S2 trials. See Fig. 2 caption for details.

the difference Error-Correct (black curve in Fig. 2 and 3) exhibits an anticipated "large positive, then small negative peak" pattern on grand averages [1, 4, 7, 11, 12], compared to the literature, both peaks seem to be delayed by approximately 100-200 ms (Fig. 4). Another, maybe more peculiar, discrepancy concerns the manifestation of profound, strong peaks also in Correct trials. In relevant works, the Error-Correct curve's average waveform seems to result from the corresponding modulation in Error trials alone, with Correct trials remaining flat [1,

Published by
Verlag der Technischen Universität Graz

10.3217/978-3-99161-014-4-093

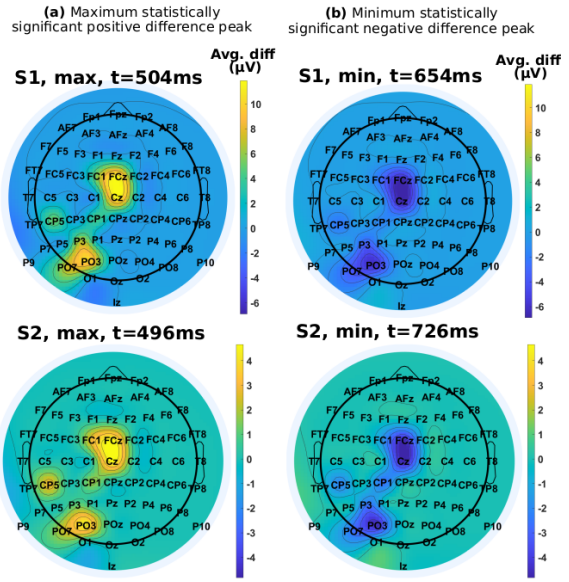

Figure 4: Topographic distribution of the average EEG amplitude difference Error-Correct within the narrow 8-channel layout used, for the maximum statistically significant positive difference peak (left) and the minimum, statistically significant negative difference peak (right) for subjects S1 (top) and S2 (bottom). Text on top of the plots specifies the exact time point where the corresponding peaks shown are located. Bright yellow indicates large positive average difference, deep blue large negative average difference, and green no average difference.

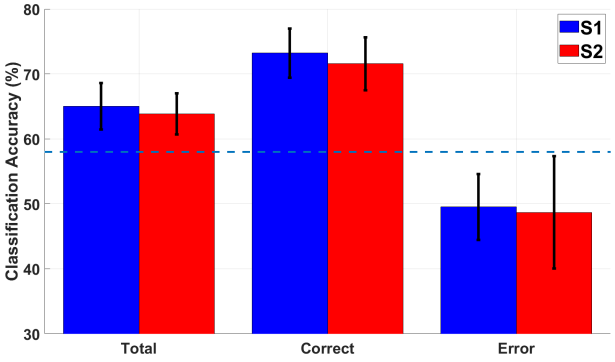

Figure 5: Average and standard deviation (across cross-validation folds) of the Total and class-wise (Correct, Error) classification accuracy for subjects S1 (blue) and S2 (red). The horizontal, dashed, light blue line marks the 58% random classification threshold [31].

12], or only reaching modest peak amplitudes [11], normally distinctly smaller than that of Error trials, an effect referred to as Correct-Response Negativity [32]. On the contrary, here we denote for both subjects a similar signature for both displaced and non-displaced target trials, whose peaks are of comparable amplitude; consequently, the Error-Correct grand average resembles that of regular interaction ErrPs solely due to the fact that ErrPs are delayed with respect to Correct potentials.

One possible explanation is that both Correct and Error patterns may receive contributions by Visually Evoked Potentials generated by the target stimulus appearances, resulting (through some complex and currently unclear process) in the observed waveform shapes. The delayed Error signature seems to somewhat align with this theory. Of note, the original target stimulus happens at a random, subject-dependent time in the interval [-0.5,0] ms before the movement onset ($t = 0$) (the trial was discarded if no movement occurred within 0.5 s after the target projection). The displaced target appearance (only for Error trials) happens at most 6 ms after $t = 0$. Hence, the derived signatures cannot be explained on the basis of Visually Evoked Potential (VEP) contributions alone. The high mental workload exerted here could also be implicated with the delayed responses.

Whatever the rationale behind the features of the ErrPs emerging in this protocol, strong peaks in Correct trials render their single-trial detection a particularly difficult task, as shown by the compromised classification accuracy obtained (yet, significantly above the random classification level overall [31]).

CONCLUSION

Our two-case study corroborates the elicitation of ErrP EEG signals in an extremely hurried eye-hand coordination task comprising “ballistic” computer mouse movements, and substantiates that the corresponding signatures are similar to the interaction ErrPs described in the relevant literature for various protocols involving EEG-monitored error processing. We show that these ErrPs can be recognized in single-trial by means of a shallow classifier, albeit accurate classification seems to be challenging. These preliminary results suggest that it may be possible to detect errors from EEG even under extremely tight time constraints of the underlying task, thus potentially enabling automatic ErrP-based error correction in rushed, real-world BCI and HCI scenarios. Future work entails confirming these results using data from all participants, delving into the mechanisms leading to this kind of novel ErrPs and improving the classification outcome leveraging the large number of subjects and trials available to apply deep and transfer learning techniques.

REFERENCES

[1] Chavarriaga R, Sobolewski A, Millán JdR. Errare machinale est: The use of error-related potentials in brain-machine interfaces. Frontiers in Neuroscience. 2014;8.

[2] Chaudhary U, Birbaumer N, Ramos-Murguialday A. Brain–computer interfaces for communication and rehabilitation. Nature Reviews Neurology. 2016;12(9):513–525.

[3] Pires G, Castelo-Branco M, Guger C, Cisotto G. Editorial: Error-related potentials: Challenges and applications. Frontiers in Human Neuroscience. 2022;16.

[4] Ferrez PW, Millán JdR. Error-related EEG potentials generated during simulated brain–computer interaction. IEEE Transactions on Biomedical Engineering. 2008;55(3):923–929.

Published by
Verlag der Technischen Universität Graz

10.3217/978-3-99161-014-4-093

[5] Hoffmann S, Falkenstein M. Predictive information processing in the brain: Errors and response monitoring. International Journal of Psychophysiology. 2012;83(2):208–212.
[6] Milekovic T, Ball T, Schulze-Bonhage A, Aertsen A, Mehring C. Error-related electrocorticographic activity in humans during continuous movements. Journal of Neural Engineering. 2012;9(2):026007.
[7] Spüler M, Niethammer C. Error-related potentials during continuous feedback: using EEG to detect errors of different type and severity. Frontiers in Human Neuroscience. 2015;9.
[8] Spüler M, Bensch M, Kleih S, Rosenstiel W, Bogdan M, Kübler A. Online use of error-related potentials in healthy users and people with severe motor impairment increases performance of a P300-BCI. Clinical Neurophysiology. 2012;123(7):1328–1337.
[9] Schmidt NM, Blankertz B, Treder MS. Online detection of error-related potentials boosts the performance of mental typewriters. BMC Neuroscience. 2012;13(1).
[10] Cruz A, Pires G, Nunes UJ. Double ErrP Detection for Automatic Error Correction in an ERP-Based BCI Speller. IEEE Transactions on Neural Systems and Rehabilitation Engineering. 2018;26(1):26–36.
[11] Bevilacqua M, Perdikis S, Millán JdR. On error-related potentials during sensorimotor-based brain-computer interface: Explorations with a pseudo-online brain-controlled speller. IEEE Open Journal of Engineering in Medicine and Biology. 2019;1:17–22.
[12] Lopes-Dias C, Sburlea AI, Müller-Putz GR. Online asynchronous decoding of error-related potentials during the continuous control of a robot. Scientific Reports. 2019;9(1).
[13] Iwane F, Iturrate I, Chavarriaga R, Millán JdR. Invariability of EEG error-related potentials during continuous feedback protocols elicited by erroneous actions at predicted or unpredicted states. Journal of Neural Engineering. 2021;18(4):046044.
[14] Iwane F, Sobolewski A, Chavarriaga R, Millán JdR. EEG error-related potentials encode magnitude of errors and individual perceptual thresholds. iScience. 2023;26(9):107524.
[15] Perdikis S, Millan JdR. Brain-machine interfaces: A tale of two learners. IEEE Systems, Man, and Cybernetics Magazine. 2020;6(3):12–19.
[16] Llera A, Gerven M van, Gómez V, Jensen O, Kappen H. On the use of interaction error potentials for adaptive brain computer interfaces. Neural Networks. 2011;24(10):1120–1127.
[17] Kim SK, Kirchner EA, Stefes A, Kirchner F. Intrinsic interactive reinforcement learning – using error-related potentials for real world human-robot interaction. Scientific Reports. 2017;7(1).
[18] Ehrlich SK, Cheng G. Human-agent co-adaptation using error-related potentials. Journal of Neural Engineering. 2018;15(6):066014.
[19] Chavarriaga R, Millan JdR. Learning from EEG error-related potentials in noninvasive brain-computer interfaces. IEEE Transactions on Neural Systems and Rehabilitation Engineering. 2010;18(4):381–388.
[20] Iturrate I, Chavarriaga R, Montesano L, Minguez J, Millán JdR. Teaching brain-machine interfaces as an alternative paradigm to neuroprosthetics control. Scientific Reports. 2015;5(1).
[21] Millan J, Mouriño J. Asynchronous BCI and local neural classifiers: an overview of the adaptive brain interface project. IEEE Transactions on Neural Systems and Rehabilitation Engineering. 2003;11(2):159–161.
[22] Iturrate I, Montesano L, Minguez J. Task-dependent signal variations in EEG error-related potentials for brain–computer interfaces. Journal of Neural Engineering. 2013;10(2):026024.
[23] Usama N, Niazi IK, Dremstrup K, Jochumsen M. Detection of error-related potentials in stroke patients from EEG using an artificial neural network. Sensors (Basel). 2021;21(18):6274.
[24] Si-Mohammed H *et al.* Detecting system errors in virtual reality using EEG through error-related potentials. In: Proceedings of the IEEE Conference on Virtual Reality and 3D User Interfaces, VR 2020. United States, Mar. 2020, 653–661.
[25] Kreilinger A, Neuper C, Müller-Putz GR. Error potential detection during continuous movement of an artificial arm controlled by brain–computer interface. Medical and Biological Engineering and Computing. 2012;50(3):223–230.
[26] Lopes Dias C, Sburlea AI, Müller-Putz GR. Masked and unmasked error-related potentials during continuous control and feedback. Journal of Neural Engineering. 2018;15(3):036031.
[27] Omedes J, Iturrate I, Minguez J, Montesano L. Analysis and asynchronous detection of gradually unfolding errors during monitoring tasks. Journal of Neural Engineering. 2015;12(5):056001.
[28] Bard C, Turrell Y, Fleury M, Teasdale N, Lamarre Y, Martin O. Deafferentation and pointing with visual double-step perturbations. Experimental Brain Research. 1999;125(4):410–416.
[29] Nitsche MA, Paulus W. Excitability changes induced in the human motor cortex by weak transcranial direct current stimulation. The Journal of Physiology. 2000;527(Pt 3):633.
[30] Daly I, Scherer R, Billinger M, Müller-Putz G. FORCe: Fully online and automated artifact removal for brain-computer interfacing. IEEE Transactions on Neural Systems and Rehabilitation Engineering. 2014;23(5):725–736.
[31] Müller-Putz G, Scherer R, Brunner C, Leeb R, Pfurtscheller G. Better than random? A closer look on BCI results. International Journal of Bioelectromagnetism. 2008;10(1):52–55.
[32] Gehring WJ, Liu Y, Orr JM, Carp J. The Error-Related Negativity (ERN/Ne). In: The Oxford Handbook of Event-Related Potential Components. Oxford University Press, Dec. 2011.

Published by
Verlag der Technischen Universität Graz